

RSC Advances



This is an *Accepted Manuscript*, which has been through the Royal Society of Chemistry peer review process and has been accepted for publication.

Accepted Manuscripts are published online shortly after acceptance, before technical editing, formatting and proof reading. Using this free service, authors can make their results available to the community, in citable form, before we publish the edited article. This *Accepted Manuscript* will be replaced by the edited, formatted and paginated article as soon as this is available.

You can find more information about *Accepted Manuscripts* in the [Information for Authors](#).

Please note that technical editing may introduce minor changes to the text and/or graphics, which may alter content. The journal's standard [Terms & Conditions](#) and the [Ethical guidelines](#) still apply. In no event shall the Royal Society of Chemistry be held responsible for any errors or omissions in this *Accepted Manuscript* or any consequences arising from the use of any information it contains.

**3² Full Factorial Design for Development and Characterization of Nanosponges Based
Intravaginal *In situ* Gelling System for Vulvovaginal Candidiasis**

AUTHORS:

Riyaz Ali M. Osmani*¹, Parthasarathi K. Kulkarni¹, S. Shanmuganathan², Umme Hani¹, Atul Srivastava¹, Prerana M³, Chetan G. Shinde¹, Rohit R. Bhosale¹,

¹Department of Pharmaceutics, JSS College of Pharmacy, JSS University, Mysuru-570 015, Karnataka, India

²Department of Pharmaceutics, College of Pharmacy, Sri Ramchandra University, Chennai- 600 116, Tamil Nadu, India

³Faculty of Life Science, JSS University, Mysuru-570 015, Karnataka, India

***CORRESPONDING AUTHOR**

Riyaz Ali M. Osmani

Research Scholar,

Department of Pharmaceutics,

JSS College of Pharmacy, JSS University,

Sri Shivarathreshwara Nagar, Mysuru-570 015, Karnataka, India.

E-mail ID: riyazosmani@gmail.com

Mobile No.: +91-8892238589

ABSTRACT

Clotrimazole (CTZ) is a BCS Class II drug having a limited therapeutic potential because of its poor aqueous solubility and a shorter half-life. The rationale behind present research effort was to enhance CTZ solubility and efficacy via forming complex with hydroxypropyl β -cyclodextrin (HP- β -CD) nanosponges. Nanosponges (NS) are hyper-cross linked cyclodextrin polymers based colloidal structures with three-dimensional networks. Herein, NS were prepared using dimethyl carbonate as a cross linker, suitably gelled and assessed for *in vitro* release, *in vitro* bioadhesion, *in vivo* antifungal activity and *in vivo* irritation using female Wistar albino rats. Nine formulations were prepared based on 3^2 full factorial design using Pluronic F-127: Pluronic F-68 ratios. The prepared CTZ-HP- β -CD NS were characterized by SEM, TEM, FT-IR spectroscopy, DSC and XRPD studies. The particle size of loaded NS (N6) was found to be 455.6 nm with least polydispersity index and high zeta potential (-21.32 ± 1.3 mV) to attain a stable colloidal nanosuspension. The optimized CTZ NS based *in situ* gel (F-10) demonstrated prolonged drug release (upto 15 h) than the conventional *in situ* gel, which got exhausted within 6 h. CTZ-NS gel depicted higher *in vivo* antifungal activity and *in vitro* bioadhesion compared to conventional *in situ* gel. Furthermore, from *in vivo* irritation studies, it could be stated that the optimized CTZ NS gel formulation was non-irritant. All these outcomes signified the promising applicability of formulated CTZ NS gel as a novel delivery system for local therapy of vaginal candidiasis and other similar infections.

KEY WORDS: Candidiasis; Clotrimazole; HP- β -CD; Nanosponges; *In situ* gel; Vaginal delivery

1. INTRODUCTION

Vaginal candidiasis is a clinical condition which is prevalent in about 75% of women for at least once in their lifetime. Among which, 80% of the infected cases are caused by the most pathogenic species from the genera *Candida* i.e. *Candida albicans*.^{1, 2} *C. albicans* is a primarily existing dimorphic fungus that is propagating through its phenotype blastophore also known as 'blastoconidia'. It is capable to transform into various morphologies like hyphae, yeast and pseudohyphae on cognizance of environmental signals; which have importance in virulence.^{3, 4} The outermost cell wall layer of the *Candida* comprises of mannoproteins with N-glycosylated polysaccharide and O-glycosylated oligosaccharide moieties. Both carbohydrate moieties have revealed to be vital in host-fungal interactions and virulence.⁵⁻⁷ The N-glycosylated polysaccharide has a comb-like structure with an α -1,6-linked backbone moiety and an oligomannose side chain chiefly comprising of α -1,2-, α -1,3-, and β -1,2-linked mannose residues with a trivial number of phosphate groups. Three types of β -1,2-linkage-containing manno-oligosaccharides is observed in the mannan. One of these is located in a phosphodiesterified oligosaccharide moiety and functions as a common epitope of *C. albicans* serotypes A.^{8, 9} *Candida albicans* J-1012 strain (serotype A) is one the prime causative organisms for vaginal candidiasis.^{1,2} The preliminary remedy to treat vulvovaginal candidiasis is the local therapy with antifungal agents. Site-specific cure is provided by the local vaginal delivery along with eluding toxic side effects of antifungal agents that are faced during oral administration. At least 5-7 days are required to treat acute vulvovaginal candidiasis, though, a concise treatment is preferred mostly and this attains better compliance. Longer treatment is needed for the effective treatments of recurrent vaginal infections.¹⁰ Antifungal imidazole derivatives are the commonly used drugs to treat fungal infections. Imidazole derivatives have lower aqueous solubility because of their

hydrophobic structure and have a negative impact on the efficacy along with raising formulation tribulations, when taken orally.¹¹ Thus, applying clotrimazole (CTZ) topically is the most commonly recommended regime for vaginal candidiasis.

An imidazole derivative, CTZ holds a wide range of anti-mycotic activity; which offers broadly efficient localized therapy with minimum risk of side effects.¹² It acts by inhibiting fungal cytochrome P450 3A enzyme (lanosine 14 α -demethylase) that governs the conversion of lanosterol to ergosterol (the chief sterol comprising fungal cell membrane). CTZ is available in numerous conventional dosage forms like ovules, gels, tablets, creams and pessaries for vaginal application. However, prolonged duration of action is not achieved because of the short residence time of these conventional dosage forms in the genitourinary tract. This compromise with the efficiency of CTZ thereby calling for multiple and frequent administration for the treatment.¹³ Moreover, CTZ is a poorly water soluble drug and this interferes with its local availability, thereby limiting the effective antifungal treatment.¹² To overcome these limitations, various delivery strategies like microemulsions, polycarbophil gels, liposomes, microspheres, nano-structured lipid carriers, cyclodextrin inclusion, sustained release bioadhesive tablets etc. have been proposed.¹⁴⁻¹⁹ However, NS potential is yet to be explored for the delivery of CTZ for improvised candidiasis therapy.

Among the recent findings are the nanosponges (NS) which are made up of microscopic particles with cavities of a few nanometers wide.^{20, 21} The lately proposed nano sized colloidal carriers particularly designed for drug delivery have potential of solubilizing drugs that are insoluble in water, proposes prolonged release, and by altering pharmacokinetic parameters they improves drug bioavailability.^{21, 22} Cyclodextrins (CDs) are used to form inclusion complexes with drug molecules for enhancing their aqueous solubility, masking unwanted characteristics,

reducing side effects and increasing their photostability or aqueous stability in pharmaceutical field. Controlled-release properties to certain active ingredients are also described to have conveyed by CDs.^{13, 20} CDs based NS are comprised of hyper-crosslinked system produced by crosslinking different CD molecules using cross linkers like carbonyl or carboxylate compounds.²³ Resulting systems formed are crosslinked polymers encompassing captivating properties like inclusion or absorption of chemicals, swelling and proficient release of active agents. When compared to other nanocarriers, NS offer high drug loading apart from validating great potential for determining concerns related to bioavailability, solubility, controlled release of a range of therapeutic agents and stability.²² Besides, NS that are prepared can be assimilated into conventional dosage forms like ointments, gels, creams, lotions and powders for resourceful applications.

Prior studies portray CD based NS as a carrier for paclitaxel, acyclovir, curcumin, camptothecin, itraconazole and other drugs.²⁴⁻²⁹ Furthermore, the ability of NS in uplifting solubility and the bioavailability of diverse molecules that include resveratrol and tamoxifen were also reported.^{21, 24}

A vital challenge in the vaginal drug delivery is patient's pliability during administration of dosage forms and following up with repeated-dose therapeutic regimen.¹³ Among various conventional formulations, gels have vital advantages like versatility, safety, higher bioavailability and being economical. Gels are tolerated in a better way by the patients compared to other dosage forms and it is understood that vaginal therapy can be vitally improvised if a delivery system can hold the drug at the site of administration for an extended period.^{10, 13} *In situ* gelling drug delivery systems release drugs in response to environmental circumstances as a result of stimulus-dependent changes in rheological properties of the polymer platform.³⁰⁻³⁶

Hence, such systems can be formulated to deliver adequate coverage of the vagina and retaining the formulation on the mucosal tissue extensively. Pluronic F-127 (PF-127) and Pluronic F-68 (PF-68) are synthetic copolymers of poly(ethylene oxide)-b-poly(propylene oxide)-b-poly(ethylene oxide) exhibiting thermoreversible behavior in aqueous solutions. The hydrophilicity and hydrophobicity of the Pluronics mainly depends on the poly ethylene oxides (PEO) to poly propylene oxides (PPO) ratio. PF-127 with an average molar mass of 12,600 g/mol, contains PEO/PPO in the ratio of 7:3. Whereas copolymer PF-68 with the molar mass of ~8400 g/mol contains 8:2 ratio of PEO/PPO.³¹ The thermoreversible behavior of Pluronics is due to the change in micellar properties as a function of both concentration of polymers and environmental temperature, and a reversible gelation may occur at physiological temperature.^{37,}³⁸ By using such systems, many benefits like high spreadability and ease of application at temperatures that are below sol-gel temperature and rheological structuring are offered to the vagina for topically administering therapeutic agents and therefore, vaginal retention at body temperature is enriched.

In this perspective, the current study for vaginal delivery of CTZ-HP- β -CD NS based *in situ* gel formulation was attempted with mucoadhesive and thermosensitive properties to confirm longer residence at the infection site, thereby providing a satisfactory release profile of CTZ for the augmented and efficient vulvovaginal candidiasis therapy.

2. MATERIALS AND METHODS

CTZ (MW: 344.837 g/mol, purity >98%) was kindly provided as a gift sample from Glenmark Pharmaceuticals Ltd., Mumbai, India. (2-hydroxypropyl)- β -cyclodextrin (~1480 g/mol) and dimethylcarbonate (90.08 g/mol) were purchased from Alfa Aesar, England and Loba

Chemie, Mumbai, India, respectively. Pluronic F-127 (PF-127, 12600 g/mol) and Pluronic F-68 (PF-68, ~8400 g/mol) were purchased from Sigma-Aldrich, St. Louis, USA. All other chemicals and reagents used were of analytical grade. Ultra-purified water was used for all experiments.

2.1. Synthesis of HP- β -CD NS

HP- β -CD based NS were prepared using dimethylcarbonate (DMC) as cross-linking agent. Different molar ratios of HP- β -CD and DMC (1:2, 1:4 and 1:8 for batches A, B and C respectively) were used to prepare NS via method previously reported by Swaminathan *et al.*²⁷ In brief; anhydrous HP- β -CD was added to DMC at about 90°C under magnetic stirring and allowed to react for 5 h. The reaction mixture was left to cool and the solid recovered by filtration. Later, obtained solid mass was broken up via gentle mortar grinding and Soxhlet assembled extraction using ethanol was done for removing unreacted DMC and other impurities. Excess amount of cross linker was used to carry out the reaction and resulting NS were stored at 25°C after purification for further usage.

2.2. CTZ incorporation in NS

Accurately weighed amount of CTZ was dispersed in aqueous suspensions of NS in diverse weight ratios (1:1A, 1:1B, 1:1C, 1:2A, 1:2B, 1:2C) and stirred magnetically for 24 h (Table 1). These suspensions were then centrifuged at 2000 rpm for 10 min to separate out the non-complexed drug as a residue below the colloidal supernatant. The colloidal supernatants were then subjected to freeze-drying using a Modulyo freeze drier (Edwards, UK) to obtain the CTZ loaded NS. Finally, the acquired NS were stored in a covered vacuum desiccator at ambient temperature for further studies.^{23, 24}

2.3. Solubilization efficiency

The CTZ solubilization efficiency of NS (for batches A, B, C) was determined using shake-flask method to evaluate solubilization enhancement capacity.¹² Briefly, two glass vials were taken; an excess quantity of CTZ was suspended in 20 ml ultra-purified water in one vial. To another vial containing a fixed quantity of HP- β -CD NS in 20 ml ultra-purified water, excess amount of CTZ was added. Both the vials were sealed and shake on a mechanical shaker (Remi, India) at ambient temperature for 24 h. Resultant suspensions were then subjected to centrifugation (5,000 rpm for 15 min via Research Compufuge, Remi PR-24 Centrifuge, Remi, India), supernatants were filtered through membrane filter (0.45 μ m, 13 mm, Pall Life Sciences, Mumbai, India) and filtrates were analyzed for concentration of dissolved CTZ by UV-spectrophotometry at 264 nm (Pharmaspec 1700, Shimadzu, Japan). The experiments were performed in triplicate ($n = 3$).

2.4. Entrapment efficiency

Entrapment or loading efficiency of CTZ was determined by quantitative estimation of drug loaded into NS. Weighed amount of CTZ-HP- β -CD NS (10 mg) were dissolve in methanol, sonicated for 15 min for breaking the complex, centrifuged, filtered supernatant was diluted suitably and then analyzed by UV-spectrophotometer at 264 nm.^{25, 39} The entrapment efficiency (%) of NS was determined using following Equation 1:

$$\text{Entrapment efficiency} = C_e/C_{th} \times 100 \quad (1)$$

Where, C_e : entrapped drug concentration; C_{th} : theoretical drug concentration

2.5. Characterization of CTZ HP- β -CD NS

2.5.1. Fourier transformed infrared (FT-IR) spectroscopy

FT-IR spectroscopy (Shimadzu 8400 S, Japan) was implied to recognize possible interaction of CTZ with NS. The spectra were obtained using KBr pellets within the range 4000 cm^{-1} to 400 cm^{-1} .

2.5.2. Differential scanning calorimetry (DSC)

Differential scanning calorimetry was performed for CTZ, physical mixture, blank NS and optimized NS formulation (N6) using Shimadzu, DSC 60 apparatus. All calorimetric measurements were completed using a high purity alpha alumina disc (empty cell) as the reference. High purity indium metal was adopted as standard for instrument calibration. In nitrogen atmosphere with a heating rate of 10 $^{\circ}\text{C}/\text{min}$, dynamic scans were taken in temperature range 10-300 $^{\circ}\text{C}$.

2.5.3. X-ray powder diffraction (XRPD)

XRD patterns of CTZ, HP- β -CD, unloaded HP- β -CD NS and CTZ loaded HP- β -CD NS were recorded at an ambient temperature using diffractometer (Rigaku, Japan). Diffraction patterns were recorded using Ni-filtered $\text{CuK}\alpha$ radiation ($\lambda = 1.5418 \text{ \AA}$), 40 kV voltage, 20 mA current and step of 0.02° for 2 sec with scan speed $0.01^{\circ}/\text{sec}$ in the interval $2\theta=10-60^{\circ}$.

2.5.4. Particle size, zeta potential, polydispersity

The average particle size and distribution, zeta potential and polydispersity index (PI) of the resulting NS were determined using Malvern Instrument (DTS Ver.5.10, MAL1031371, Malvern, UK). The experiments were performed using clear disposable zeta cell, using water as a dispersant which has refractive index (RI)-1.330 and viscosity (cP)-0.73 at 25 $^{\circ}\text{C}$ temperature constant.

2.5.5. Scanning electron microscopy (SEM)

The morphology and surface topography of prepared NS were examined using scanning electron microscope (Zeiss EVO LS 15, Smart SEM 5.05, Germany) operating at an acceleration voltage 15 kV and suitable magnification at room temperature. In brief, samples were mounted onto 5 mm silicon wafers and sputter coating was done with Au under an argon atmosphere.

2.5.6. Transmission electron microscopy (TEM)

The size and shape of NS were evaluated by means of transmission electron microscope (Philips CM 10) assembled with NIH image software. Suspensions (with 0.5% w/v concentration) of CTZ loaded or unloaded NS were sprayed uniformly on Formvar-coated copper grids, and were observed after complete air-drying.

2.6. Formulation of NS based CTZ gel

PF-127 and PF-68 served as gelling agents and gel was prepared according to the classical 'cold method'.⁴⁰ The Pluronic F-127 (18-22 % w/w) and Pluronic F-68 (5-15 % w/w) polymers were added into pre-cooled ultra-purified water (4 °C) with continuous agitation. The solutions were then kept in a refrigerator overnight (4 °C) to ensure complete dissolution and pH was adjusted to neutral using triethanolamine. CTZ NS (drug equivalent to 200 mg) were incorporated into the gel (10 g) to get 2% w/w CTZ. Conventional gel was made in the same way; instead of NS, free CTZ was incorporated. The prepared gels were packed in glass vials and sealed until further use.

2.7. Preparation of simulated vaginal fluid (SVF)

SVF was prepared from 3.51 g/L sodium chloride, 1.40 g/L potassium hydroxide, 0.222 g/L calcium hydroxide, 2 g/L lactic acid, 0.018 g/L bovine serum albumin, 0.4 g/L urea, 1 g/L acetic acid, 0.16 g/L glycerol and 5 g/L glucose. The pH of the mixture was adjusted to 4.5 ± 0.02 using 0.1M hydrochloric acid.¹⁹

2.8. Experimental design

Experimental design is a systematic and scientific approach to study the relationship and interaction between independent and dependent variables. A 2-factor, 3-level full factorial design (3^2) was employed for optimizing CTZ-HP- β -CD NS based *in situ* gels using DESIGN EXPERT® (version 9.0.5) software available from Stat-Ease Inc., Minneapolis, MN. The concentration of PF-127 (A) and PF-68 (B) were optimized by using Design of Experiment (DoE) at three different levels: low (-1), medium (0) and high (+1). Gelation temperature ($^{\circ}\text{C}$) (R1); gelation time (sec) (R2) and *in vitro* drug release (% cumulative drug release) (R3) were selected as response variables (Table 2). A statistical model incorporating interactive and polynomial terms was utilized to evaluate the formulation responses; Equation (2).

$$Y = b_0 + b_1A + b_2B + b_3AB + b_4A^2 + b_5B^2 \quad (2)$$

Where, Y is the response, b_0 is the arithmetic mean response of the 9 runs. The responses in the above equation Y are the quantitative effect of formulation components or independent variables A and B; b_0 is the arithmetic mean response; b_1 , b_2 , b_3 , b_4 and b_5 are the estimated coefficient for the factors A and B. Details of the factorial design are given in the Table 2. The prepared gels were characterized and evaluated for sol-gel transition, gelation temperature, gelation time, *in vitro* drug release, pH, drug content, viscosity, spreadability, *in vitro* bioadhesion, *in vivo* fungal activity and *in vivo* irritation.

2.9. Characterization of CTZ NS gel

2.9.1. Gelation temperature

The gelation temperature of NS based thermosensitive *in situ* gel (5 ml) was estimated by heating it in a thin walled glass tube (internal diameter-10 mm, length-82 mm, thickness-0.6

mm) placed in a temperature controlled water bath with gentle shaking till it is converted to gel. The temperature of water was increased at a rate of 2 °C/5 min constantly. Gel formation was taken as the point where there was no flow when the test tube was inverted. This temperature was noted as gelation temperature.⁴¹

2.9.2. Gelation time

Gelation time of NS based *in situ* gel was determined by tube inversion method. 5 ml NS based *in situ* gel was taken in a thin-walled glass tube having same geometry/specifications as mentioned above. The gelation time was measured at the respective gelation temperature noted earlier. The filled glass tube was immersed in the temperature-controlled water bath adjusted to the respective gelation temperature. The test tube was taken out at regular intervals and inverted to observe physical state of the sample. The gelation time was determined by a flow or no-flow criterion with the test tube inverted. Time taken by the system to gel i.e. flow to no flow was noted as gelation time.⁴²

2.9.3. In vitro release studies

The *in vitro* drug release studies were performed using Franz diffusion cell (Perme Gear Inc., Bethlehem, PA) with donor chamber and water jacketed receptor chamber (20 ml) maintained at 37°C. Commercial semipermeable cellophane membrane (Fischer Scientific Co., London, England; pore size 0.45 µm) was used as permeation barrier; which was soaked overnight in SVF before the study. 1 g of gel was placed carefully on cellophane membrane; which was placed between the donor and receptor compartments. Receptor compartment contained 20 ml SVF, while donor compartment was empty and open to atmosphere. The contents of receptor section were balanced at 37±5 °C with continuous stirring at rate 25 rpm, on a magnetic stirrer. Aliquots (5 ml) were withdrawn at regular intervals from receptor

compartment and equal volume of fresh receptor medium (37 ± 5 °C) was replaced to maintain the sink condition. Withdrawn samples were analyzed by UV-spectrometer at 264 nm. The study was conducted in triplicate.

2.9.4. pH

The pH of prepared 2% (w/w) gel was determined using a digital pH meter (Mettler Toledo MP 220, Greifensee, Switzerland) at 25 °C in triplicate.

2.9.5. Drug content

The drug content was determined using 1 g of NS based *in situ* gel in 100 ml volumetric flask, dissolved in methanol and after appropriate dilutions, analyzed by UV-spectrophotometry as quoted earlier.^{39, 43}

2.9.6. Viscosity studies

Viscosity measurements of the formulated NS based *in situ* gel was carried out using Brookfield viscometer (DV-II, LV model, Brookfield, USA) using small volume adaptor with a thermo stated water jacket and SC4-18 spindle. The viscosity was measured ($n=3$) at three temperatures viz. at 4°C, 25°C and 37°C at different rotational speeds from 0.5-20 rpm with a torque of near to 100%. The samples were equilibrated for 10 min before the measurement; also the instrument was equipped with a temperature control unit.^{31, 44}

2.9.7. Spreadability

One of the criteria for a gel to meet the ideal qualities is that it should possess good spreadability. It is the term expressed to denote the extent of area to which gel readily spreads on application site. The spreadability was determined using a method previously reported by Bachhav *et al.*³⁹ The spreadability was evaluated by placing 0.5 g gel within a premarked circle of 1 cm diameter on a glass plate with specifications of 5 mm thickness and 15 cm² area. Another

glass plate with similar dimensions was placed over it; care has been taken to avoid entrapment of the air bubbles between two slides. Weight of 500 g was kept on the upper glass plate for 5 min to spread the gel uniformly. The increase in the diameter due to spreading of the gel was noted as an indicator of spreadability.

2.9.8. *In vitro* bioadhesion studies

In vitro bioadhesive potential of CTZ loaded NS gel was evaluated and compared with plain CTZ gel, as reported formerly by Bachhav *et al.*¹² Briefly, an agar plate (1%, w/w) was prepared in pH 4.5 citrate phosphate buffer and test sample (50 mg) was placed at its center. After five minutes, plate was assembled with USP disintegration test apparatus and ran in up-down motions in SVF (pH 4.5) at 37 ± 1 °C. The motion of instrument arm was such that the sample on the plate was immersed into solution at the lowest point and was taken out of solution at the highest point. The residence time of test samples on plate was noted by visual observation.

2.9.9. *In vivo* antifungal activity

In vivo experimental procedures including handling, were approved by the Institutional Animal Ethics Committee (Registration No. 144/2013) complied with the guidelines set out by the Committee for the Purpose of Control and Supervision of Experiments on Animals (CPCSEA), Animal Welfare Division, Ministry of Environment and Forests, Government of India, India.

18 healthy female Wistar albino rats (150-200 g, 6-8 weeks) were used for the assessment of *in vivo* performance of CTZ NS gel. Two days prior to vaginal inoculation, all animals were maintained under pseudoestrus by subcutaneous injection of estradiol valerate (25 mg/kg). Before starting the experiments, vaginal cultures of all animals were performed and no *Candida sp.* were noted. In these oophorectomized rats, *C. albicans* (10^7 blastoconidia/ml in 20 μ l of

sterile saline solution) were inoculated. Administration was done using a tuberculin syringe devoid of needle.

From each animal vaginal fluid was taken using a sterile swab after every 2 days. These swabs were then streaked on a Sabouraud dextrose agar (SDA) plates and were incubated (LHC-78-Labhospmake, India) at 35°C for 72 h. At least one vaginal sample was evaluated for each animal and inoculums viability was established by counting number of colony forming units (CFUs) via a serial dilution method. The infected animal subjects were divided into three groups: GF1: control group with no treatment, GF2: received plain CTZ gel and GF3: received optimized NS gel formulation (F3) designed to treat vaginal candidiasis.

The respective gel samples (for GF2 and GF3) were singly applied in vagina using an injector without a needle.

For evaluating vaginal burden, samples were collected by rolling a sterile cotton swab over the vaginal cavity. Swabs were then streaked over Sabouraud dextrose agar (SDA) plates and incubated (LHC-78-Labhospmake, India) for 3 days at 35°C, prior to analysis. The vaginal swabs were collected on 1st, 3rd, 5th, 7th, 14th and 21st days after administering formulations intravaginally. After 21 days, the animals were sacrificed by an excess dose of pentobarbital and vaginal tissues were excised. The vaginal tissues were fixed in 10% neutral buffered formalin, dehydrated in a graded alcohol series, cleared with methyl benzoate and embedded in paraffin wax. The histopathological studies were done via light microscopy by taking tissue sections (4 µm), stained with haematoxylin and eosin (HE) and vaginal inflammation was investigated by observing neutrophil accumulation. Grading scores have been assigned as low, moderate or

extensive depending on inflammatory infiltrate, fibrosis and lamina propria infiltration by inflammatory cells.

2.9.10. *In vivo* irritation studies

The vaginal irritation potential of plain CTZ and CTZ NS *in situ* gels were evaluated by a method reported by Francois *et al.*⁴⁵

9 healthy female Wistar albino rats (150-200 g, 6-8 weeks) were used for the *in vivo* irritation studies and were evaluated for vaginal/vulval irritation, bleeding or discharge from vagina prior to studies. Animals were divided into three groups ($n = 3$) as:

Group GI1: control group with no treatment,

Group GI2: administered plain CTZ *in situ* gel and,

Group GI3: administered CTZ NS *in situ* gel.

The formulations were administered (0.25 ml/kg) by a 1 ml plastic syringe. After application, vaginal cavity was observed for any signs of possible irritation of the vaginal mucosa (i.e., erythema and edema) and related mucosal reactions for 3 days. The mean erythematous scores were recorded (0-4) on the basis of degree of erythema as: 0 = no erythema, 1 = slight erythema (barely perceptible light pink), 2 = moderate erythema (dark pink), 3 = moderate to severe erythema (light red) and 4 = severe erythema (extreme redness). The experimental animals were sacrificed and transverse section of the vaginal tissue was scrutinized by experienced pathologist for the severity of atrophy and epithelial loss.

3. RESULTS AND DISCUSSION

3.1. Solubilization efficiency

The solubilization efficiency studies revealed potential of HP- β -CD NS in enhancing CTZ solubility. The percentage solubilization of CTZ by NS was observed in order

C(1:8)>B(1:4)>A(1:2) as depicted in Fig. 1. The solubilization enhancement factor observed for NS batches A, B, and C was 9 ± 0.03 , 17 ± 0.02 and 32 ± 0.06 , respectively. The increase in solubility of CTZ was due to matrix entrapment and formation of inclusion complexes. The major factor affecting the extent of inclusion complex formation was the degree of crosslinking between NS and CTZ. Higher the degree of crosslinking among NS and CTZ, higher will be the drug entrapment/loading and inclusion complexation; consequently leading to enhanced solubilization.⁴⁶ Moreover, increased solubilization of NS could be attributed to possible masking of CTZ hydrophobic groups, decreased crystallinity and increased wetting behavior as reported in earlier findings.^{23, 29}

3.2. Entrapment efficiency

The entrapment efficiency of NS formulations was found to be in the range of 15.34 ± 0.49 to 85.12 ± 0.61 (Table 1). The entrapment efficiency was observed in order of $N6>N3>N5>N2>N4>N1$. The highest loading of N6 NS formulation (85.12%) compared to other formulations could be attributed to highest crosslinking between HP- β -CD and DMC; which permits the encapsulation of CTZ in the inner structure of NS. The difference in entrapment of CTZ showed that degree of cross-linking affected the complexation capacity of NS. As observed in N1, the lower amount of crosslinker formed a network with an incomplete cyclodextrin cross-linking, with decreased sites for CTZ complexation; thus, CTZ not included in higher amount. However, in N6, higher amount of cross-linker provides high cross-linking of HP- β -CD, and consequently higher CTZ interaction with HP- β -CD cavities leads to better entrapment as reported previously by Ansari *et al.*⁴⁷ and Shende *et al.*⁴⁸ Based on promising solubilization and entrapment efficiency NS formulation N6 was chosen as optimized formulation and used for further studies.

3.3. Characterization of CTZ-HP- β -CD NS

3.3.1. FT-IR studies

The comparison of FT-IR spectra of pure CTZ, unloaded NS and CTZ loaded HP- β -CD NS is depicted in Fig. 2. The spectrum of CTZ (Fig. 2A) showed all characteristic absorption peaks, as at 3057 cm^{-1} (aromatic C-H stretch), 1597 cm^{-1} (aromatic C=N stretch of imidazole ring), 1423 cm^{-1} (aromatic C=C stretch of imidazole ring), 1082 cm^{-1} and 1016 cm^{-1} (aromatic C-N stretch of imidazole ring), 1215 cm^{-1} and 1278 cm^{-1} (in-plane C-H bend) and 912 cm^{-1} , 845 cm^{-1} and 767 cm^{-1} (out of plane C-H bend).¹⁹ FT-IR spectrum of unloaded HP- β -CD NS (Fig. 2B) showed characteristic absorption band at 3400-2800 cm^{-1} due to O-H stretching vibrations of HP- β -CD and the presence of carbonate bond which has a peak at around 1728 cm^{-1} ; which indicates formation of CD based NS, as previously reported.^{27, 49} In addition, the other characteristics peak of unloaded NS were found at 2929 cm^{-1} due to C-H stretching vibration, 1361 cm^{-1} of C-H bending vibration and 1018 cm^{-1} corresponding to C-O stretching vibration of primary alcohol.

In spectrum of CTZ loaded HP- β -CD NS (Fig. 2C) due to interaction of CTZ with NS, all sharp peaks belonging to the HP- β -CD NS have appeared but were shifted to higher or lower wave number, i.e. 1726-1734 cm^{-1} , 1424-1401 cm^{-1} , 1027-1030 cm^{-1} and only few characteristics peak of CTZ were visible at 1064 cm^{-1} , 1020 cm^{-1} , 962 cm^{-1} , 750 cm^{-1} and 528 cm^{-1} confirming definite interaction between CTZ and NS.

3.3.2. DSC studies

DSC is an extremely valuable tool in NS thermal behavior investigation and it offers physicochemical state information of drug loaded in NS both qualitatively and quantitatively. The DSC thermograms of CTZ, CTZ NS physical mixture, unloaded HP- β -CD NS and CTZ

loaded HP- β -CD NS are shown in Fig. 3. DSC analysis of pure CTZ (Fig. 3A) resulted in gradual enthalpy change producing a linear sharp endothermic peak at temperature 147.47°C which is indicative of its melting temperature.⁵⁰ This endothermic peak was also traced in respect of NS physical mixture (Fig. 3B) but with lesser intensity. While in case of blank NS a broad peak appeared around 95.27°C corresponding to HP- β -CD (Fig. 3C) as reported earlier by Sinha *et al.*⁵¹ However, DSC thermogram of the CTZ loaded HP- β -CD NS (Fig. 3D) did not show the melting peak due to formation of inclusion and non-inclusion complex between NS and CTZ. Drug peak disappearance in DSC thermogram of NS was mainly because the drug got encapsulated, molecularly dispersed in NS structure and was unable to crystallize; which confirmed the interaction between CTZ and NS, as previously alluded by Rao *et al.*⁵²

3.3.3. XRPD studies

To characterize physical nature of CTZ within the NS and to evaluate the mode of interaction amongst CTZ and NS, X-ray powder diffraction of CTZ, HP- β -CD, CTZ NS physical mixture and CTZ loaded HP- β -CD NS were done. Encapsulation in HP- β -CD NS alters the crystallinity of the drug by changing it to an amorphous state losing its crystallinity, as previously reported by Shende *et al.*⁴⁸ The XRD pattern of pure CTZ (Fig. 4A) presented intense, sharp diffraction peaks indicating its crystalline nature, at 2θ of 10.3°, 12.4°, 18.6°, 19.5°, 20.7° and several minor peaks at 14.2°, 16.7°, 18.8°, 19.9°, 24.4°, 27.5°, 28.2° as reported earlier.¹⁹ XRPD pattern of HP- β -CD (Fig. 4B) showed absence of sharp diffraction peaks but presence of a broad peak in the range of 2θ 20-30°; confirming its amorphous structure as previously reported by Wang *et al.*⁵³ Further, the appearance of sharp peaks of the drug indicated retention of the crystalline structure of CTZ in the NS physical mixture (Fig. 4C). However, smaller intensity of some peaks of CTZ could be due to the diluting effect of HP- β -CD.¹⁹ CTZ

crystallinity reduced subsequent to NS encapsulation; which consequently led it to amorphous nature and thus disappearance of crystalline peaks in XRPD pattern of CTZ loaded HP- β -CD NS (Fig. 4D), as stated earlier by Rao *et al.*⁵² These findings proved that drug interaction complexation was not just because of components mechanical mixing; which lie in great agreement with FT-IR and DSC results.

3.3.4. Particle size, zeta potential, polydispersity

The average diameter, polydispersity index and zeta potential of CTZ-HP- β -CD NS (N6) were found to be 455.6 ± 11 nm, 0.143 and -21.32 ± 1.3 mV respectively (Table 3). Zeta potential of CTZ NS were found sufficiently high probably due to presence of the carbonate groups in its structure which ensure physical stability between NS particles through electrostatic repulsion, and thereby avoiding aggregations.⁵⁴

3.3.5. SEM, TEM analysis

NS size and surface morphology were further investigated using SEM and TEM analysis. NS were found to be roughly spherical in shape with spongy nature^{39, 48} and uniform distribution via outcomes of both. SEM micrograph depicting the surface morphology of NS (Fig. 5) reflected that formed NS were having numerous fine surface voids; probably as a result of solvent diffusion. Also no residual, intact crystals of CTZ were seen on NS surface, indicating that NS matrix being formed by CTZ-HP- β -CD. TEM results explored that regular size and shape of blank HP- β -CD NS were unaffected even after CTZ loading as shown in Fig. 6. Furthermore, as explained by Shende *et al.* the extra porous nature of NS might be due to encapsulation of drug in between NS structure.⁵⁴

3.4. Characterization of CTZ NS gel

NS embedded thermosensitive *in situ* gel was prepared to increase viscosity, residence time and for improving localization of CTZ in vaginal cavity. Nine formulations of CTZ-HP- β -CD NS based *in situ* gel (F-1 to F-9) were prepared as per full factorial design (Table 2) by changing two independent variables, concentration of PF-127 (A) and PF-68 (B). Table 4 shows the response values R1: gelation temperature ($^{\circ}\text{C}$); R2: gelation time (sec); R3: *in vitro* drug release studies (% cumulative drug release) and were subjected to multiple regressions to yield polynomial equations, coefficient values indicate the effect by changing individual variable; 3D response surface graphs and contour plots were constructed.

3.4.1. Gelation temperature

The prepared CTZ NS based *in situ* gel exhibited temperature-dependent reversible sol-to-gel transition. When these systems were evaluated for gelation temperature studies, the *in situ* gel systems transformed from sol-to-gel at a temperature less than body temperature. The formulations showed gelation temperature in range of 26.9 ± 0.33 $^{\circ}\text{C}$ to 38.8 ± 0.23 $^{\circ}\text{C}$. Based on 3^2 factorial designs, the factor combinations of A and B resulted in different response variables for gelation temperature (R1). The equation derived by best fit mathematical model to relate the response R1 and factors (A, B) was $R1 = +32.900 - 3.683A - 2.250B$. ANOVA of the equation suggested the model F value 1829.07, P value < 0.0001 ; indicating that the model is significant. The increase or decrease effects of response on different level combination of independent variables are indicated by a positive or negative sign of the polynomial terms. As the predicted r^2 0.9963 is in reasonable concurrence with adjusted r^2 0.9978, the above polynomial equation showed a good fit of response variables at different levels. 3D surface plot of R1 is portrayed in Fig. 7A showed a significant decrease in gelation temperature with an increase in factors A and

B. The gelation temperature of the developed system was found to be concentration dependent; higher is the concentration of PF-127 and PF-68, higher is its thermoresponsivity. There was no significant effect of factor A and B interaction on the gelation temperature.

3.4.2. Gelation time

Being an *in situ* vaginal gel drug delivery system, along with the sol-gel transition at physiological conditions, another prerequisite is to form gel within an optimum time. Fast sol-gel transition is required to hold the *in situ* NS gel and ultimately the drug in the vaginal cavity so as to give a prolonged localized drug release. The results of gelation time indicated that prepared CTZ NS based *in situ* gel quickly responded to variation in gelation temperature. The gelation temperature and time were mainly evaluated for comparing the prepared formulation batches and to find out a final optimized formulation. The formulations were subjected to their respective gelation temperatures; which resulted in quick gelation in less than 61 ± 1 sec. The gelation time of all the formulation was found within the range 43 ± 1 to 61 ± 1 sec. Based on 3^2 factorial designs, the factor combinations of A and B resulted in different response variables for gelation time (R2). The equation derived by best fit mathematical model to relate the response R2 and the independent variables was $R2 = +51.333 - 5.500A - 4.000B$. ANOVA of the equation suggested the model F value 128.08, P value < 0.0001 indicating that the model is significant. Also, the predicted r^2 0.9442 is in reasonable concurrence with adjusted r^2 0.9695. Gelation time was significantly influenced by the factors A and B. Increase in the polymers concentration led to decreased gelation time for around 18 sec. 3 Dimensional response (3D) plot of R2 is represented in Fig. 7B showed a significant decrease in gelation time with an increase in factors A and B. This might be due to increased viscosity of the system at an increasing level of factors A and B.

3.4.3. *In vitro* release studies

In vitro drug release studies provide vital information about pretended performance of the formulation during *in vivo* conditions. The results of *in vitro* release studies indicated that drug release was prolonged. The equation derived for R3 by best fit mathematical model was: $R3 = +78.052 - 11.250A - 7.936B$ with predicted r^2 0.9490 in reasonable agreement with adjusted r^2 0.9715. It was found that the effect of factor A is more significant than factor B; with an increase in factor A release rate of CTZ from *in situ* vaginal gels significantly decreased. Prolonged CTZ release from formulations up to 12 h was mainly influenced by the factor A. In addition, the factor B has contributed for better performance of factor A in terms of quick gelation time and lower gelation temperature. ANOVA of the equation suggested the model F value 137.32, P value <0.0001 indicating that the model is significant. Dimensional response (3D) plot of R3 is portrayed in Fig. 7C showed a significant decrease in drug release with an increase in A and B. All formulations exhibited prolonged release of CTZ devoid of any burst release. Drug release from NS was due to gradual erosion of NS and concomitant diffusion of drug into the external polymer matrix. The prolonged release from NS gels is of great interest for enhancing vaginal drug delivery and maintaining the required concentration for overall treatment of vulvovaginal candidiasis.

3.4.4. Check point analysis and optimization of design

To optimize all the responses with different targets, a multi-criteria decision approach (a numerical optimization technique by the desirability function and a graphical optimization technique by the overlay plot) was used (Fig. 8A). The optimized *in situ* gel formulation (F-10) was obtained by applying constraints as $R1 = 34$ °C, $R2 = 53$ sec, $R3 = 82\%$ on responses. These constraints were common for all the formulations. Recommended concentrations of the factors

were calculated by the DoE from above plots which has highest desirability near to 1.0. The optimum values of selected variables obtained using DoE was 19.448 % of A and 9.811% of B. Desirability and overlay plot of DoE gave optimum values of both factors, from that final formulation was prepared. The optimized gel formulation (F-10) was prepared for check point analysis and evaluated for gelation temperature ($^{\circ}\text{C}$), gelation time (sec), *in vitro* drug release (% cumulative drug release) up to 12 h, which showed response variable as $R_1=33.7\pm 0.61$ $^{\circ}\text{C}$; $R_2=52\pm 1$ sec; $R_3=80.37\pm 0.59\%$. There is a close agreement between predicted and observed values (Table 5) proved by desirability value of 0.991 with low relative errors (Fig. 8B). It demonstrated the reliability of the optimization procedure followed in the present study to prepare formulation as per 3^2 factorial designs. Factors A and B with the composition of 19.5% and 9.9% are suitable for drug delivery as NS based *in situ* vaginal gel, and thus chosen for CTZ NS based *in situ* gel delivery in this study.

Fig. 9A shows the *in vitro* release profiles of plain CTZ gel and optimized CTZ NS based *in situ* gel (F-10). The release profile indicated that drug entrapped within the NS gel was not released completely at the end of 12 h (80.37%). The release data from NS based *in situ* gel was fitted into various kinetic models. The value of r^2 was found to be highest for the Higuchi model ($r^2 = 0.92$); which indicates that the test product follows matrix-diffusion-based release kinetics. No initial burst release was observed in release profile of optimized CTZ NS gel, confirmed that CTZ was not adsorbed on NS surface and well encapsulated within nanostructures. These results were in good agreement with earlier findings of Swaminathan *et al.*²⁷ A similar sustained release profile was obtained with camptothecin polyrotaxane-based delivery systems, molecularly assembled using CDs.⁵⁵

3.4.5. pH, drug content

The pH of optimized formulation (F-10) was found to be 4.57 that is equivalent with vaginal pH. The drug content of the formulation (F-10) was noted to be $97.83 \pm 0.26\%$ of the theoretical value (2% w/w). The drug content value implied that the drug was significantly loaded in the NS based *in situ* gel.

3.4.6. Viscosity studies

For thermosetting gels, the viscosity at various conditions is an important rheological parameter involved in its utilization and *in vivo* performance. For instance, if viscosity is too high it will lead to difficult instillation; on the contrary, if viscosity is too low it will give rise to increased drainage. An ideal *in situ* vaginal gel should be less viscous liquid at room temperature so as to allow easy administration into the site of application; where it undergoes *in situ* phase transition to form a strong gel with enhanced viscosity.^{31, 56} PF-68 alone caused to form weaker gel bases, while the high concentration of PF-127 polymer gives the hardest gel. Solutions containing less than 15% PF-127 did not form gels, whereas a PF-127 concentration higher than 25% led to difficulty in preparation and administration.⁵⁶⁻⁵⁸ In this context combination of PF-127 and PF-68 had been used in the present study.

Viscosity of CTZ NS based *in situ* gel was measured at 4°C, 25°C and 37°C representing the storage, room and body temperature respectively. Viscosity studies of gel revealed a temperature dependent increase in viscosity. The viscosity of the optimized formulation at 4°C and 25°C was recorded as 326 cps and 1143 cps; however a significant increase in viscosity (201700 cps) was noted at 37°C, which can be attributed to sol-gel conversion. Pluronics being non-ionic PPO triblock copolymers aggregate into micelles at 37°C; which result from the dehydration of polymer blocks with temperature. It has been revealed that the gel formation

results from micellar enlargement, and hence they cannot be separated easily from each other, which accounts for the greater viscosity and rigidity of gels.^{31, 59, 60} Gelation temperature ($T_{sol-gel}$) is the temperature at which the liquid phase makes a transition to gel with sudden increase in viscosity. In the present study, optimized formulation exhibited a gelation temperature of $33.7 \pm 0.61^\circ\text{C}$.

3.4.7. Spreadability

Spreadability is an important property of semisolid formulations, affecting the ease of application and patient compliance. The *in situ* gel with a good spreadability will take less time to spread which ultimately leads to ease of application. In the present study, spreadability is expressed in terms of increased diameter (6.6 cm) of a formerly drawn circle (1 cm) as a result of applied weight. In case of optimized gel (F-10) the overall increase in diameter was found to be 7.6 cm; reflecting good spreadability.

3.4.8. *In vitro* bioadhesion studies

When two materials (both biological, or a biological and a synthetic) are held together by interfacial forces for extended period of time, they depict phenomenon called bioadhesion.⁶¹ Mostly when interaction occurs between any polymer and epithelial surface; it is referred to as bioadhesion. With reference to bioadhesive drug delivery systems, bioadhesion typically refers to the adhesion between soft tissues and polymers, either natural or synthetic.^{62, 63} Evaluation of bioadhesion is important to ensure that the adhesion offered by formulations is sufficient to ensure prolonged retention at the site of application, but not excessively so, as this may be associated with damage to the mucous membrane. The bioadhesive potential of CTZ NS based vaginal gel and plain CTZ gel were evaluated by *in vitro* method and found to be 53 ± 2.5 min and 38 ± 1.2 min respectively ($n = 3$). The bioadhesive potential of formulated *in situ* gels could be

attributed to the fact that Pluronics with hydrophilic oxide group binds to oligosaccharide chains of mucosal membrane.^{57, 64, 65} Higher concentrations of PF-127 could therefore provide more number of hydrophilic oxide groups which ultimately binds to oligosaccharide chains, likely to prolong the residence time at the absorption site. Addition of PF-68, which is a homologue of PF-127, enhanced the bioadhesive force, since PF-68 also contains 80% of hydrophilic oxide groups. Moreover, the retention time depicted by NS gel was found to be higher with respect to plain CTZ gel. These results evidently reflect that CTZ-HP- β -CD NS based vaginal gel may have greater residence time in vaginal cavity in comparison with plain gel. Similar results were earlier reported for bioadhesion of econazole nitrate by Esra *et al.*¹⁰

3.4.9. *In vivo* antifungal activity

The mechanism of action of CTZ is by inhibiting fungal cytochrome P-450 enzyme causing hindrance in biosynthesis of ergosterol; which decreases fungal cell wall integrity.⁶⁶ The pattern of fungal clearance kinetics graph is shown in Fig. 9B. Results were found to be encouraging for the prepared CTZ NS based gel, when compared to plain CTZ gel. The vaginal swab samples were taken on 1st, 3rd, 5th, 7th, 14th and 21st days after treatment. The vaginal swabs of untreated control group of animals were observed positive for *C. albicans* up to the 21st day, however, striking disparity in fungal clearance kinetics of plain CTZ gel and CTZ NS based gel was observed. CTZ NS based gel reflected an accelerated clearance, while least clearance was noted with plain CTZ gel.

The biocompatibility of CTZ NS *in situ* gel was assessed by histopathological studies. It was observed that the fungal infection was consistent in control group (GF1). In case of plain CTZ *in situ* gel (GF2) moderate evidence of inflammation was observed, whereas optimized CTZ NS *in situ* gel (GF3) presented low signs of inflammation. The grading scores noted for GF1, GF2 and GF3 were as extensive inflammation (10/10), moderate inflammation (6/10) and low inflammation (1/10),

respectively. Inflammatory and non-inflammatory micrographs of vaginal mucosa are shown in Fig. 10.

3.4.10. *In vivo* irritation studies

In vivo vaginal irritation studies were carried out for evaluating the tolerability of CTZ NS based *in situ* gel after administration. It was observed that plain CTZ (GI2) and CTZ NS based *in situ* gel (GI3) were well tolerated by the rats with no signs of erythema and/or edema (erythema score 0) even after 3 days.^{67, 68} However, the control group (GI1) showed severe erythema (erythema score 4).

4. CONCLUSIONS

Our study proved that the solubility and efficacy of CTZ was enhanced by loading in NS, a biocompatible cross linked cyclodextrin polymer. All characterization results confirmed the interaction and formation of inclusion complex of CTZ with NS. Incorporation of CTZ NS in *in situ* vaginal gel executed therapeutically better effects than the conventional formulation. The higher solubilization and prolonged release of CTZ from CTZ NS serves the purpose of synthesizing NS. Moreover, *in vitro* bioadhesion and *in vivo* antifungal activity revealed higher residence time and improved potential of CTZ NS gel to alleviate vaginal infection more effectively than conventional formulation. The prepared cyclodextrin based CTZ loaded NS gel might be proposed as a promising carrier for an effective and superior local treatment for vaginal candidiasis.

ACKNOWLEDGEMENTS

The authors express deep sense of gratitude towards Central Food Technological Research Institute (CFTRI), Mysuru (a constituent laboratory of CSIR, New Delhi) and JSS University, Mysuru for provision of obligatory facilities to carry out present research work.

AUTHOR'S STATEMENT

Conflict of Interest

The authors declare no any conflict of interest.

REFERENCES

1. U. Hani, R. S. Bhat and H. G. Shivakumar, *Lat Am J Pharm.* 2011, **30**, 161-167.
2. M. A. B. Guzel, *Crit Rev Microb.* 2011, **37**, 250-261.
3. T. Kourkoumpetis, D. Manolakaki, G. Velmahos, Y. Chang, H. B. Alam, M. M. De Moya, E. A. Sailhamer, and E. Mylonakis, *Virulence*, 2010, **1**, 359-366.
4. J. W. van der Meer, F. L. van de Veerdonk, L. A. Joosten, B. J. Kullberg, and M. G. Netea, *Int J Antimicrob Agents*, 2010, **36**, 58-62.
5. T. Kanbe and J. E. Cutler, *Infect Immun.* 1994, **62**, 1662-1668.
6. C. Timpel, S. Strahl-Bolsinger, K. Ziegelbauer and J. F. Ernst, *J. Biol. Chem.* 1998, **273**, 20837-20846.
7. C. A. Munro, S. Bates, E. T. Buurman, H. B. Hughes, D. M. MacCallum, G. Bertram, A. Atrih, M. A. Ferguson, J. M. Bain, A. Brand and S. Hamilton, *J. Biol. Chem.* 2005, **280**, 1051-1060.
8. F. Dalle, T. Jouault, P. A. Trinel, J. Esnault, J. M. Mallet, P. d'Athis, D. Poulain and A. Bonnin, *Infect Immun.* 2003, **71**, 7061-7068.
9. N. Shibata, H. Kobayashi, Y. Okawa and S. Suzuki, *Eur J Biochem.* 2003, **270**, 2565-2575.
10. E. Baloglu, S. Y. Karavana, Z. A. Senyigit, S. Hilmioglu-Polat, D. Y. Metin, O. Zekioglu, T. Guneri and D. S. Jones, *J Pharm Pharmacol.* 2011, **63**, 1274-1282.
11. U. Hani, H. G. Shivakumar, R. Vaghela, R. A. M. Osmani and A. Shrivastava, *Infect Disord Drug Targets* 2015, **15**, 42-52.
12. Y. G. Bachhav and V. B. Patravale, *AAPS Pharm Sci Tech.* 2009, **10**, 476-481.

13. E. Bilensoy, M. A. Rouf, I. Vural, M. Sen and A. A. Hincal, *AAPS Pharm Sci Tech.* 2006, **7**, E1-E7.
14. K. Knuth, M. Amiji and J. Robinson, *Adv Drug Deliv Rev.* 1993, **11**, 137-167.
15. J. L. Richardson, J. Whetstone, A. N. Fisher, P. Watts, N. F. Farraj and M. Hinchcliffe, *J Control Release.* 1996, **42**, 133-142.
16. M. W. Joraholmen, Z. Vanic, I. Tho and N. Skalko-Basnet, *Int J Pharm.* 2014, **472**, 94-101.
17. E. Szymanska, K. Winnicka, A. Amelian and U. Cwalina, *Chem Pharm Bull (Tokyo).* 2014, **62**, 160-167.
18. L. Ravani, E. Esposito, C. Bories, V. L. Moal, P. M. Loiseau, M. Djabourov, R. Cortesi and K. Bouchemal, *Int J Pharm.* 2013, **454**, 695-702.
19. U. Hani, G. Krishnab and H. G. Shivakumara, *RSC Adv.* 2015, **5**, 35391-35404.
20. R. A. Osmani, R. R. Bhosale, U. Hani, R. Vaghela, P. K. Kulkarni, *Curr Drug Ther.* 2015, **10**, 3-19.
21. R. A. Osmani, U. Hani, R. R. Bhosale, P. K. Kulkarni and S. Shanmuganathan, *Curr Drug Targets* 2015, E-pub ahead of print.
22. T. Gursalkar, A. Bajaj and D. Jain. *Acta Pharm.* 2013, **63**, 335-358.
23. S. Swaminathan, P. Vavia, F. Trotta and S. J. Torne, *J Incl Phenom Macrocycl Chem.* 2007, **57**, 89-94.
24. D. Lembo, S. Swaminathan, M. Donalizio, A. Civra, L. Pastero, D. Aquilano, P. Vavia, F. Trotta and R. Cavalli, *Int J Pharm.* 2013, **443**, 262-272.
25. S. J. Torne, K. A. Ansari, P. R. Vavia, F. Trotta and R. Cavalli, *Drug Deliv.* 2010, **17**, 419-425.

26. B. Mognetti, A. Barberis, S. Marino, G. Berta, S. D. Francia and F. Trotta, *J Incl Phenom Macrocycl Chem.* 2012, **74**, 201-210.
27. S. Swaminathan, L. Pastero, L. Serpe, F. Trotta, P. Vavia, D. Aquilano, M. Trotta, G. Zara and R. Cavalli, *Eur J Pharm Biopharm.* 2010, **74**, 193-201.
28. G. Hariri, A. D. Edwards, T. B. Merrill, J. M. Greenbaum, A. E. Ende and E. Harth, *Mol Pharmaceutics* 2014, **11**, 265-275.
29. S. S. Darandale and P. R. Vavia, *J Incl Phenom Macrocycl Chem.* 2013, **75**, 315-322.
30. Y. Kim, B. Shin, V. K. Garripelli, J. Kim, E. Davaa, S. Jo and J. Park, *Eur J Pharm Sci.* 2010, **41**, 399-404.
31. E. A. Ibrahim, S. Ismail, G. Fetih, O. Shaaban, K. Hassanein and N. H. Abdellah, *Acta Pharm.* 2012, **62**, 69-70.
32. M. A. Mirza, S. Ahmad, M. N. Mallick, N. Manzoor, S. Talegaonkar and Z. Iqbal, *Colloids Surf B Biointerfaces.* 2013, **103**, 275-282.
33. R. R. Pereira, J. S. Ribeiro Godoy, T. I. Stivalet Svidzinski and M. L. Bruschi, *J Pharm Sci.* 2013, **102**, 1222-1234.
34. Y. Liu, Y. Y. Zhu, G. Wei and W. Y. Lu, *Eur J Pharm Sci.* 2009, **37**, 306-312.
35. P. Patel and P. Patel, *Int J Pharm Investig.* 2015, **5**, 50-56.
36. S. Y. Karavana, S. Rencber, Z. A. Senyigit, E. Baloglu, *Pharmacol Pharm.* 2012, **3**, 417-426.
37. D. S. Jones, M. L. Bruschi, O. Freitas, M. P. D. Gremiao, E. H. G. Lara and G. P. Andrews, *Int J Pharm.* 2009, **372**, 49-58.

38. C. G. Shinde, T. M. Pramodkumar, M. P. Venkatesh, K. S. Rajesh, A. Srivastava, R. A. M. Osmani and Y. Sonawane, *RSC Adv.* 2016, accepted manuscript DOI: 10.1039/C5RA22672D.
39. Y. G. Bachhav and V. B. Patravale, *Int J Pharm.* 2009, **365**, 175-179.
40. N. Patel, V. Thakkar, P. Moradiya, T. Gandhi and M. Gohel, *J Drug Deliv Sci Technol.* 2015, **29**, 55-69.
41. T. Vohra, I. Kaur, H. Heer and R.R. Murthy, *Cancer Nanotechnol.* 2013, **4**, 1-12.
42. M. P. Venkatesh, T. M. Kumar, B. S. Avinash and G. S. Kumar, *Curr Drug Deliv.* 2013, **10**, 188-197.
43. Y.K. Lin, Z.R. Huang, R.Z. Zhuo and J.Y. Fang, *Int. J. Nanomedicine*, 2010, **5**, 117-128.
44. R.A.M. Osmani, N.H. Aloorkar, D.J. Ingale, P.K. Kulkarni, U. Hani, R.R. Bhosale and D.J. Dev, *Saudi Pharm J.* 2015, **23**, 562-572.
45. M. Francois, E. Snoeckx, P. Putteman, F. Wouters, E. D. Proost, U. Delat, J. Peeters and M. E. Brewser, *AAPS Pharm Sci.* 2003, **5**, E5.
46. A. A. Olteanu, C. Arama, C. Radu, C. Mihaescu and C. Monciu, *J Incl Phenom Macrocycl Chem.* 2014, **80**, 17-24.
47. K. A. Ansari, P. R. Vavia, F. Trotta and R. Cavalli, *AAPS Pharm Sci Tech.* 2011, **12**, 279-286.
48. P. K. Shende, F. Trotta, R. S. Gaud, K. Deshmukh, R. Cavalli and M. Biasizzo, *J Incl Phenom Macrocycl. Chem.* 2012, **74**, 447-454.
49. M. Ramirez-Ambrosi, F. Caldera, F. Trotta, L. A. Berrueta and B. Gallo, *J Incl Phenom Macrocycl Chem.* 2014, **80**, 85-92.

50. S. Prodduturi, K. L. Urman, J. U. Otaigbe and M. A. Repka, *AAPS Pharm Sci Tech.* 2007, **8**, E152-E161.
51. V.R. Sinha, A. Nanda, R. Chadha and H. Goel. *Acta Poloniae Pharmaceutica-Drug Res.* 2011, **68**, 585-592.
52. M. Rao, A. Bajaj, I. Khole, G. Munjapara and F. Trotta, *J Incl Phenom Macrocycl Chem.* 2013, **77**, 135-145.
53. J. Wang, Y. Cao, B. Sun and C. Wang, *Food Chem.* 2011, **127**, 1680-1685.
54. P. Shende, K. Deshmukh, F. Trotta and F. Caldera, *Int J Pharm.* 2013, **456**, 95-100.
55. C. Moon, Y. Kwon, W. Lee, Y. Park, L. Chang and V. Yang, *J Biomedical Mat Res Part A* 2008, **84**, 238-246.
56. J. Y. Chang, Y. K. Oh, H. G. Choi, Y. B. Kim and C. K. Kim, *Int J Pharm.* 2002, **241**, 155-163.
57. H. G. Choi, J. H. Jung, J. M. Ryu, S. J. Yoon, Y. K. Oh and C. K. Kim, *Int J Pharm.* 1998, **165**, 33-44.
58. A. A. Koffi, F. Agnely, G. Ponchel and J. L. Grossiord, *Eur J Pharm Sci.* 2006, **27**, 328-335.
59. A. Cabana, A. Ait-Kadi and J. Juhasz, *J Colloid Interface Sci.* 1997, **190**, 307-312.
60. N. Jain, V. Aswal, P. Goyal and P. Bahadur, *J Phys Chem.* 1998, **102**, 8452-8460.
61. R. Sareen, S. Kumar and G. D. Gupta, *Curr Drug Deliv.* 2011, **8**, 407-415.
62. S. K. Roy and B. Prabhakar, *Trop J Pharm Res.* 2010, **9**, 91-104.
63. C. Valenta, *Adv Drug Deliv Rev.* 2005, **57**, 1692-1712.
64. C. S. Yong, J. S. Choi, Q. Z. Quan, J. D. Rhee, C. K. Kim, S. J. Lim, K. M. Kim, P. S. Oh and H. G. Choi, *Int J Pharm.* 2001, **226**, 195-205.

65. J. Y. Jaiswal and Mehta K, *Int J Pharm Pharm Sci.* 2011, **3**, 96-102.
66. R. A. Osmani, N. H. Aloorkar, A. S. Kulkarni, P. K. Kulkarni, U. Hani, S. Thirumaleshwar and R. R. Bhosale, *Curr Drug Deliv.* 2015, **12**, 504-512.
67. H. M. Aldawsari, S. M. Badr-Eldin, G. S. Labib and A. H. El-Kamel, *Int J Nanomedicine* 2015, **10**, 893-902.
68. A. Chatterjee, L. Kumar, B. B. Bhowmik and A. Gupta, *Pharm Dev Technol.* 2011, **16**, 466-473.

List of Tables

Table 1: Formulation batches and entrapment efficiency of CTZ loaded NS.

Table 2: Different combinations of CTZ NS based *in situ* gels using 3^2 factorial designs.

Table 3: Particle size and zeta potential of NS.

Table 4: 3^2 factorial design layout and responses noted for CTZ NS based *in situ* gels.

Table 5: Check point analysis of optimized formulation (F-10) of CTZ NS based *in situ* gel.

Table 1: Formulation batches and entrapment efficiency of CTZ loaded NS.

CTZ-NS batch code	Drug (CTZ): blank NS batch (A/B/C) [#]	Entrapment efficiency (%) [*]
N1	1:1A	15.34±0.49
N2	1:1B	51.46±0.91
N3	1:1C	74.23±0.74
N4	1:2A	39.76±0.83
N5	1:2B	62.89±1.19
N6	1:2C	85.12±0.61

[#]A, B and C stands for blank NS prepared using 1:2, 1:4 and 1:8 (HP-β-CD: dimethylcarbonate) ratios respectively.

^{*}Mean ± SD, *n* = 3

Table 2: Different combinations of CTZ NS based *in situ* gels using 3^2 factorial designs.

Formulation Code	Coded factor levels		
	A	B	
F-1	-1	-1	-1
F-2	0	-1	-1
F-3	-1	1	1
F-4	1	-1	-1
F-5	1	1	1
F-6	-1	0	0
F-7	0	0	0
F-8	0	1	1
F-9	1	0	0
Factors and their coded levels	-1	0	1
A: PF-127 amount (%)	18	20	22
B: PF-68 amount (%)	5	10	15

Table 3: Particle size and zeta potential of NS.

Formulation	Average diameter \pm	Zeta potential \pm SD*	Polydispersity
	SD* (nm)	(mV)	index
HP- β -CD NS	449.3 \pm 14	-21.61 \pm 2.1	0.141
CTZ loaded HP- β -CD NS (N6)	455.6 \pm 11	-21.42 \pm 1.3	0.143

*Mean \pm SD, $n=3$

Table 4: 3² factorial design layout and responses noted for CTZ NS based *in situ* gels.

Formulation	A [#]	B [#]	R1 [#]	R2 [#]	R3 [#]
Code			(°C)*	(sec)*	(% cumulative release)*
F-1	-1	-1	38.8±0.23	61±1	97.81±1.22
F-2	0	-1	35.2±0.22	55±1	84.93±2.13
F-3	-1	1	34.1±0.43	52±2	79.82±1.67
F-4	1	-1	31.4±0.11	49±1	73.38±1.43
F-5	1	1	26.9±0.33	43±1	61.21±2.03
F-6	-1	0	36.6±0.57	58±1	91.33±1.39
F-7	0	0	33.1±0.46	52±1	79.65±0.42
F-8	0	1	30.9±0.34	46±2	67.47±0.92
F-9	1	0	29.1±0.64	46±1	66.87±3.32

#A: concentration of PF-127, B: concentration of PF-68, R1: gelation temperature, R2:

gelation time and R3: *in vitro* drug release

*Mean ± SD, *n* = 3

Table 5: Check point analysis of optimized formulation (F-10) of CTZ NS based *in situ* gel.

Parameters	A	B	R1 (°C)	R2 (sec)	R3 (%)	Desirability
Predicted	19.448	9.811	34	53	81.45	0.991
Observed	19.5	9.9	33.7±0.61	52±1	80.37±0.59	-
Relative error	0.052	0.089	0.3	1	1.08	-
Other evaluation parameters						
			Viscosity (cps)		Drug content (%)	
			At 4°C	At 25°C	At 37°C	
			326	1143	201700	97.83±0.26

List of Figures:

Fig. 1. Comparison of CTZ solubilization by NS batches with different HP- β -CD: crosslinker ratios- A (1:2), B (1:4) and C (1:8).

Fig. 2. FT-IR spectra of (A) CTZ, (B) unloaded HP- β -CD NS and (C) CTZ loaded HP- β -CD NS.

Fig. 3. DSC thermograms of (A) CTZ, (B) physical mixture of CTZ and HP- β -CD, (C) blank HP- β -CD NS and (D) CTZ loaded HP- β -CD NS.

Fig. 4. X-ray diffractograms of (A) CTZ, (B) HP- β -CD, (C) physical mixture of CTZ and HP- β -CD, and (D) CTZ-HP- β -CD NS.

Fig. 5. Scanning electron micrograph of CTZ-HP- β -CD NS (A) at 1 KX magnification and (B) at 2 KX magnification.

Fig. 6. TEM images of (A) blank HP- β -CD NS and (B) CTZ loaded HP- β -CD NS at 46,000X.

Fig. 7. Response surface plots of (A) R1: Gelation temperature ($^{\circ}$ C); (B) R2: Gelation time (sec) and (C) R3: *In vitro* drug release (% cumulative drug release) up to 12 h at different levels of factor A and B.

Fig. 8. (A) Overlay plot for optimization of CTZ NS based *in situ* gel and (B) Contour plot represent overall desirability function of optimized formulation (F-10).

Fig. 9. (A) *In vitro* release profiles of plain CTZ and CTZ loaded HP- β -CD NS based *in situ* vaginal gels in SVF. (mean \pm S.D, $n = 3$), (B) Fungal clearance kinetics of *C. albicans* infection in infected, oophorectomized rats; each curve represents the mean of six rats. Marked differences in the fungal clearance kinetics of CTZ-HP- β -CD NS gel and plain CTZ gel have been noted ($P < 0.003$).

Fig. 10. Representative H and E (hematoxylin and eosin) stained histological slides of vaginal mucosa from female Wistar albino rats (A) Inflammatory condition with extensive neutrophil accumulation in lamina propria of the vaginal squamous epithelium and (B) Non-inflammatory vaginal mucosa in high view appearance (magnification: X200).

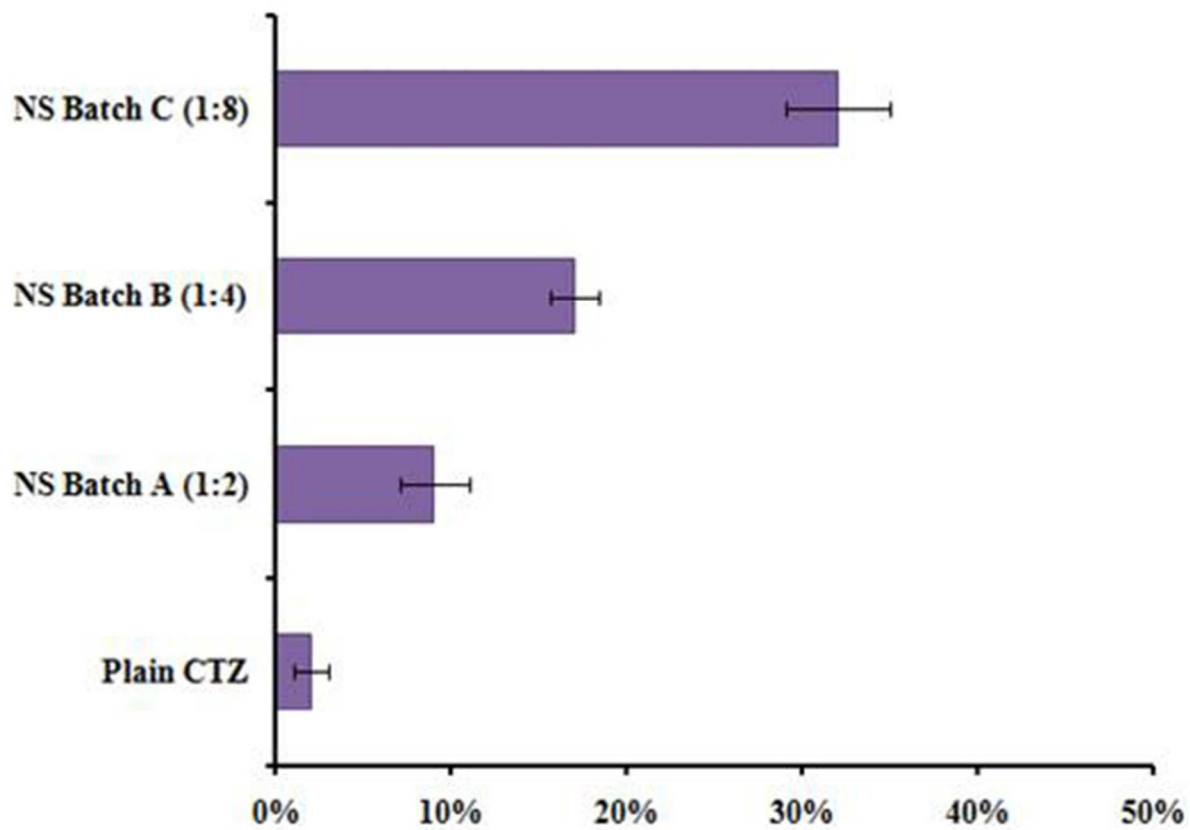


Fig. 1. Comparison of CTZ solubilization by NS batches with different HP-β-CD: crosslinker ratios- A (1:2), B (1:4) and C (1:8).

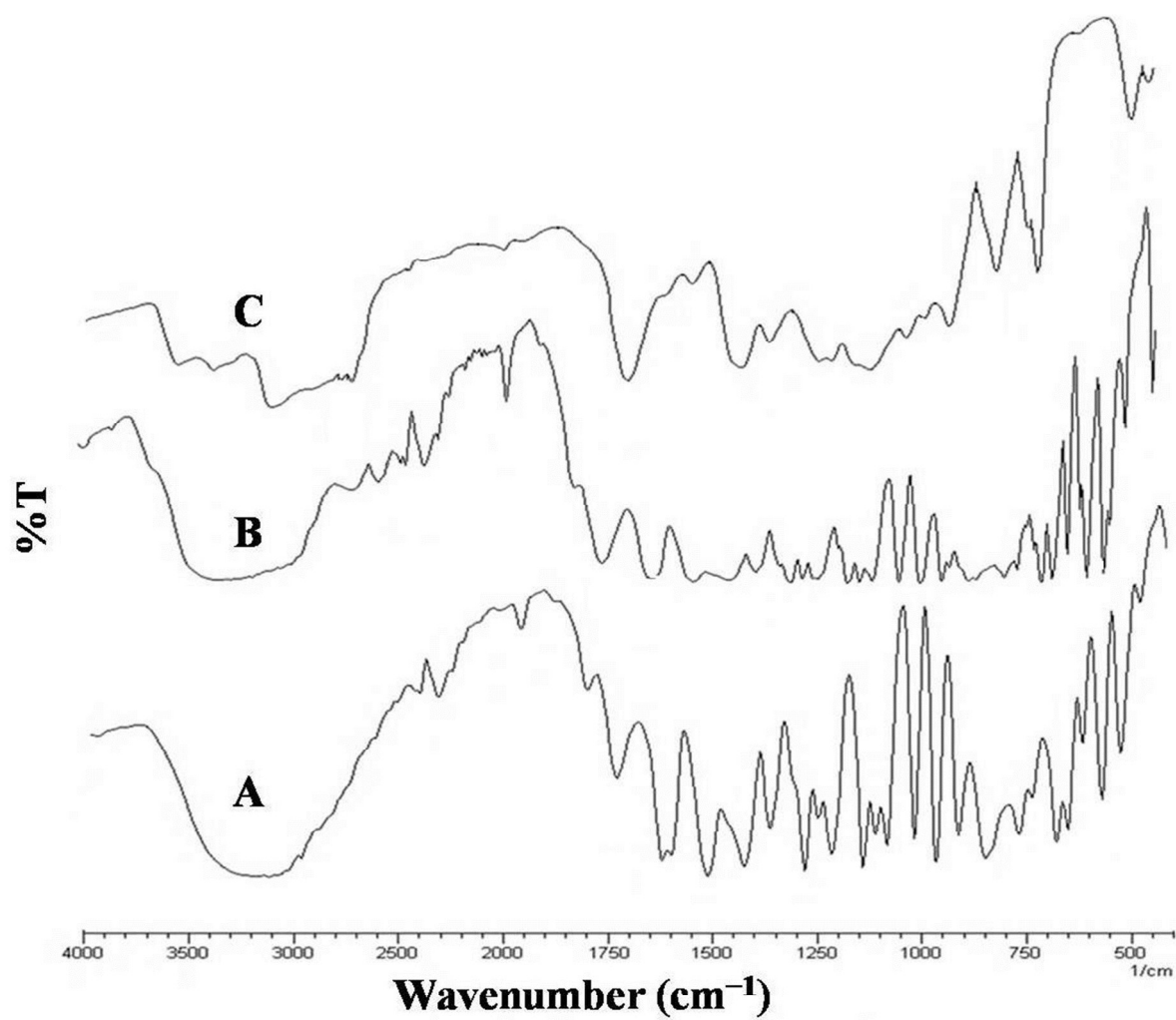


Fig. 2. FT-IR spectra of (A) CTZ, (B) unloaded HP- β -CD NS and (C) CTZ loaded HP- β -CD NS.

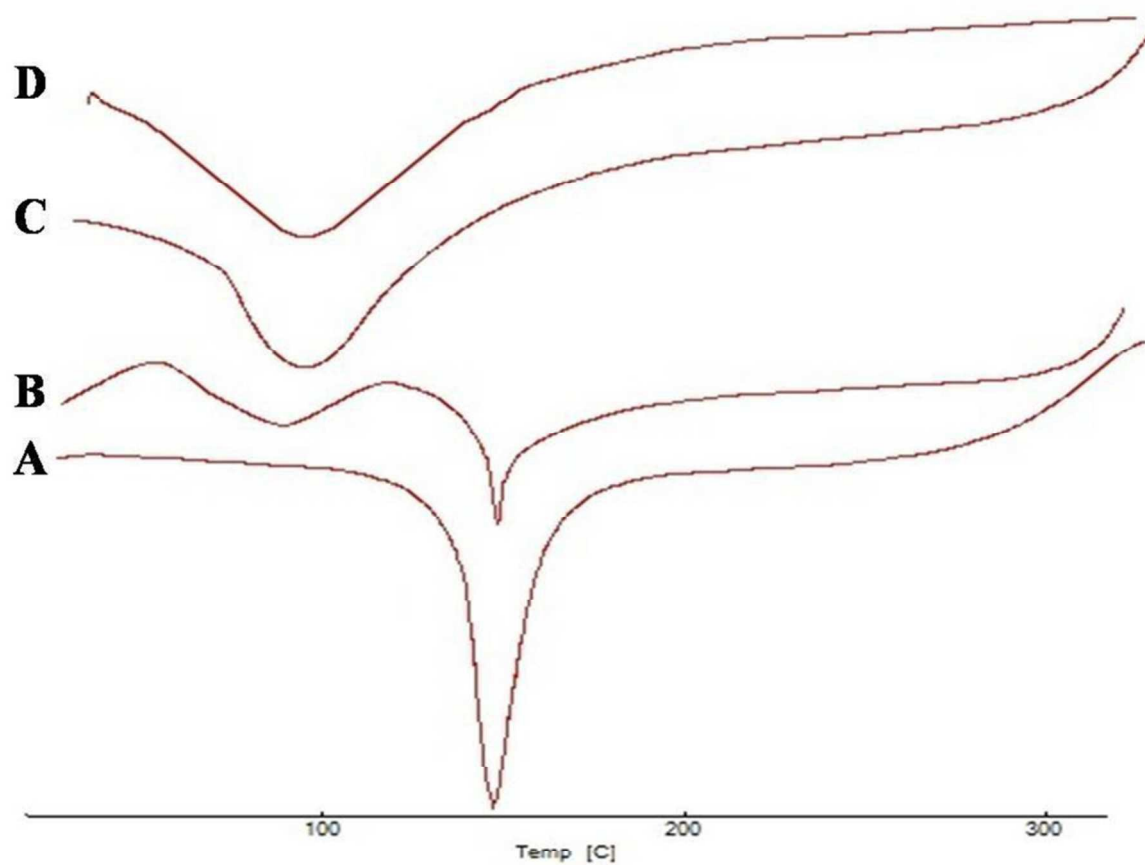


Fig. 3. DSC thermograms of (A) CTZ, (B) physical mixture of CTZ and HP-β-CD, (C) blank HP-β-CD NS and (D) CTZ loaded HP-β-CD NS.

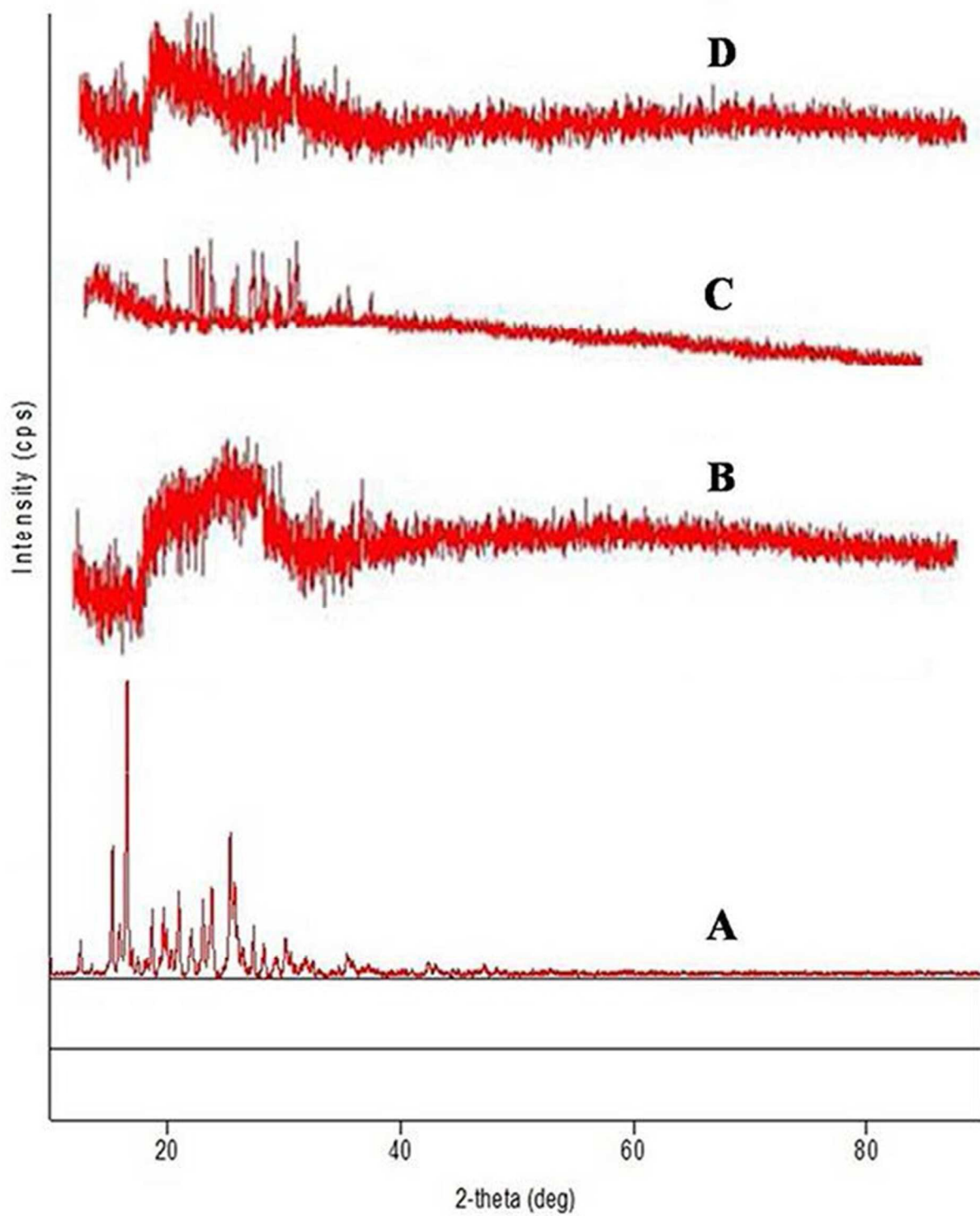


Fig. 4. X-ray diffractograms of (A) CTZ, (B) HP- β -CD, (C) physical mixture of CTZ and HP- β -CD, and (D) CTZ-HP- β -CD NS.

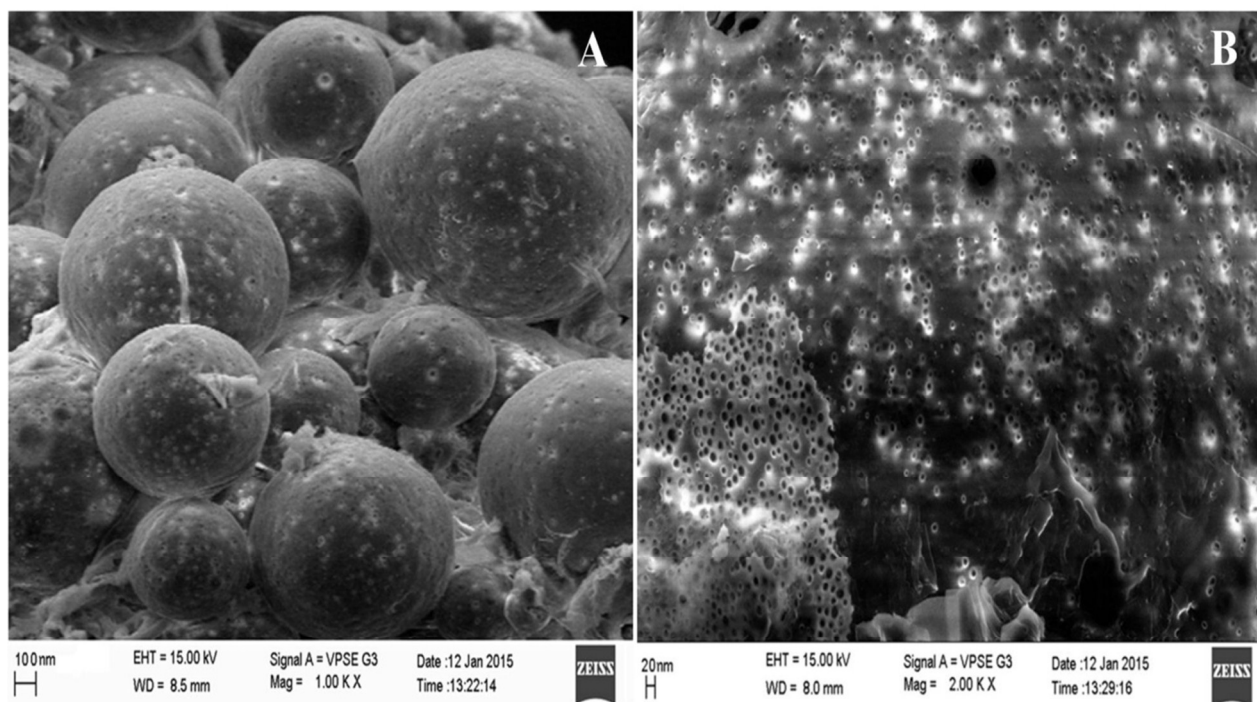


Fig. 5. Scanning electron micrograph of CTZ-HP-β-CD NS (A) at 1 KX magnification and (B) at 2 KX magnification.

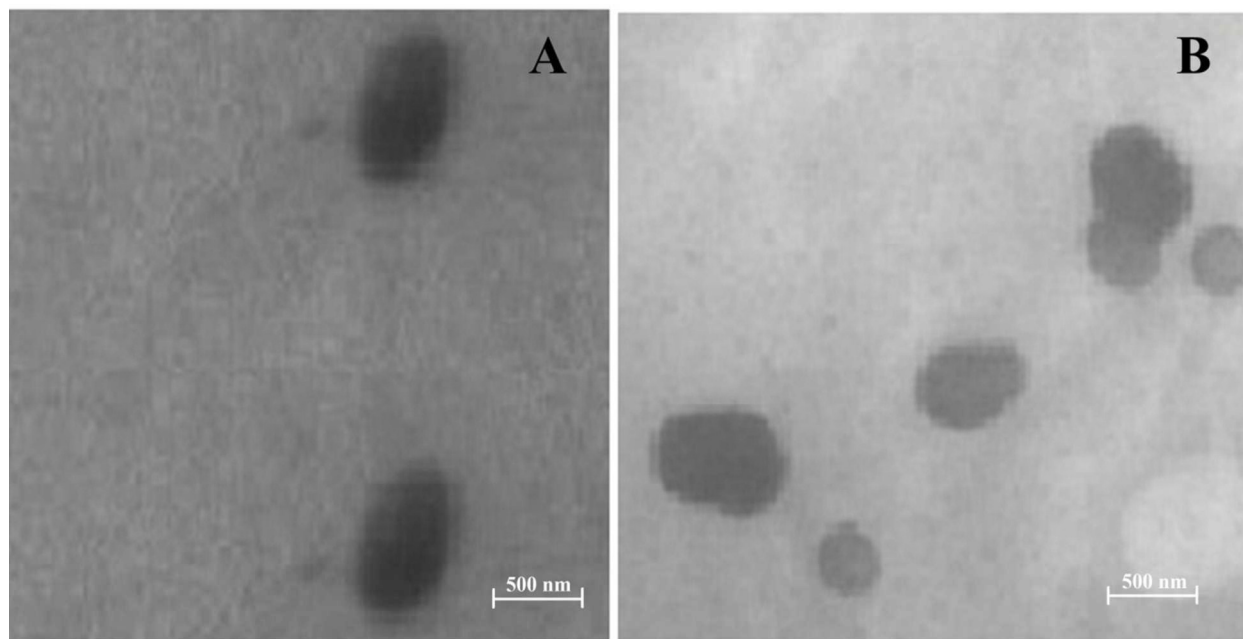


Fig. 6. TEM images of (A) blank HP- β -CD NS and (B) CTZ loaded HP- β -CD NS at 46,000X.

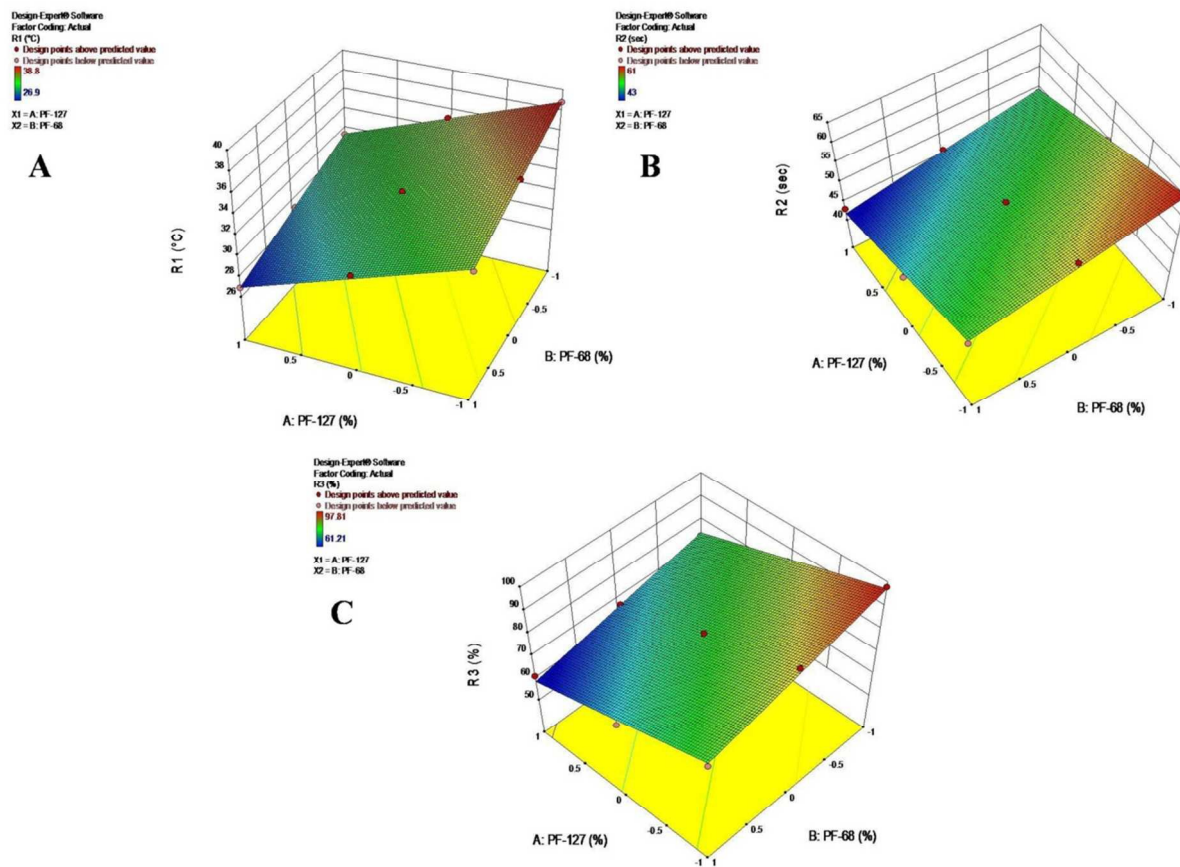


Fig. 7. Response surface plots of (A) R1: Gelation temperature (°C); (B) R2: Gelation time (sec) and (C) R3: *In vitro* drug release (% cumulative drug release) up to 12 h at different levels of factor A and B.

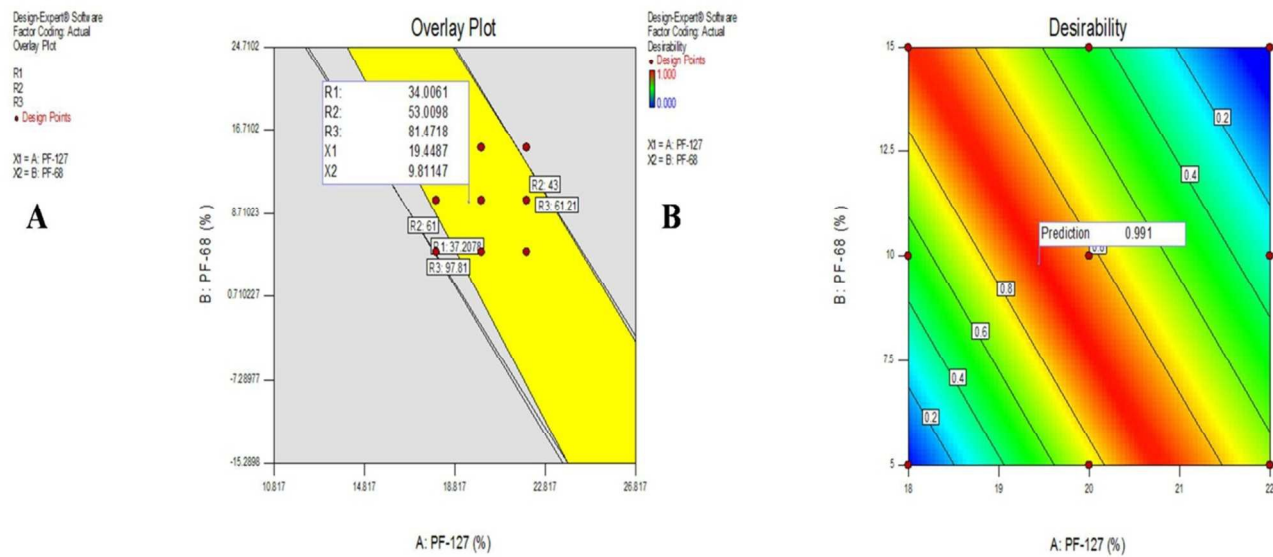


Fig. 8. (A) Overlay plot for optimization of CTZ NS based *in situ* gel and (B) Contour plot represent overall desirability function of optimized formulation (F-10).

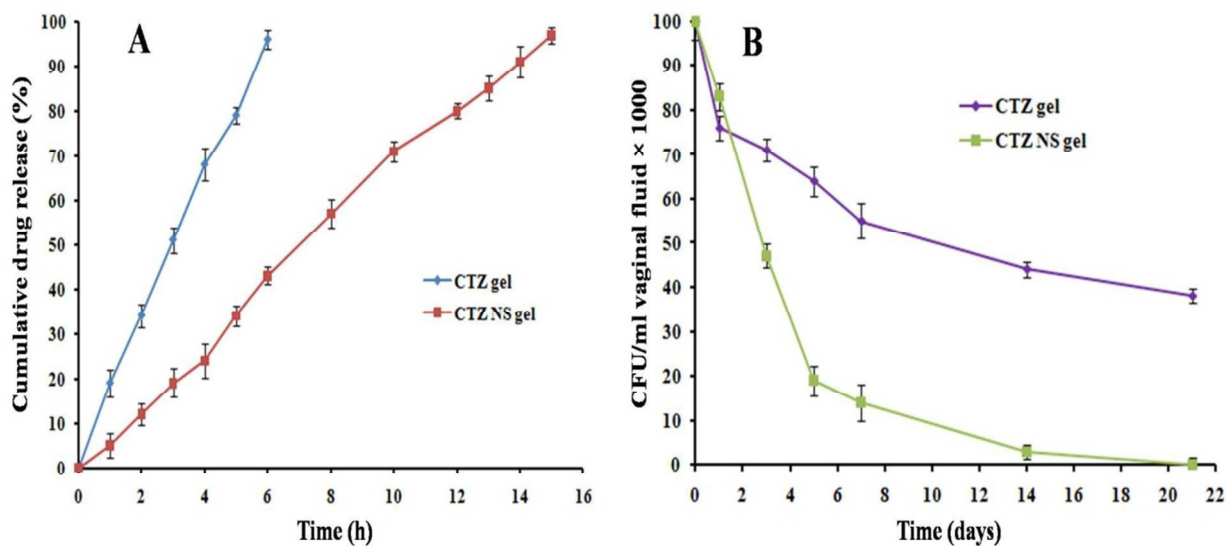


Fig. 9. (A) *In vitro* release profiles of plain CTZ and CTZ loaded HP- β -CD NS based *in situ* vaginal gels in SVF. (mean \pm S.D., $n = 3$), (B) Fungal clearance kinetics of *C. albicans* infection in infected, oophorectomized rats; each curve represents the mean of six rats. Marked differences in the fungal clearance kinetics of CTZ-HP- β -CD NS gel and plain CTZ gel have been noted ($P < 0.003$).

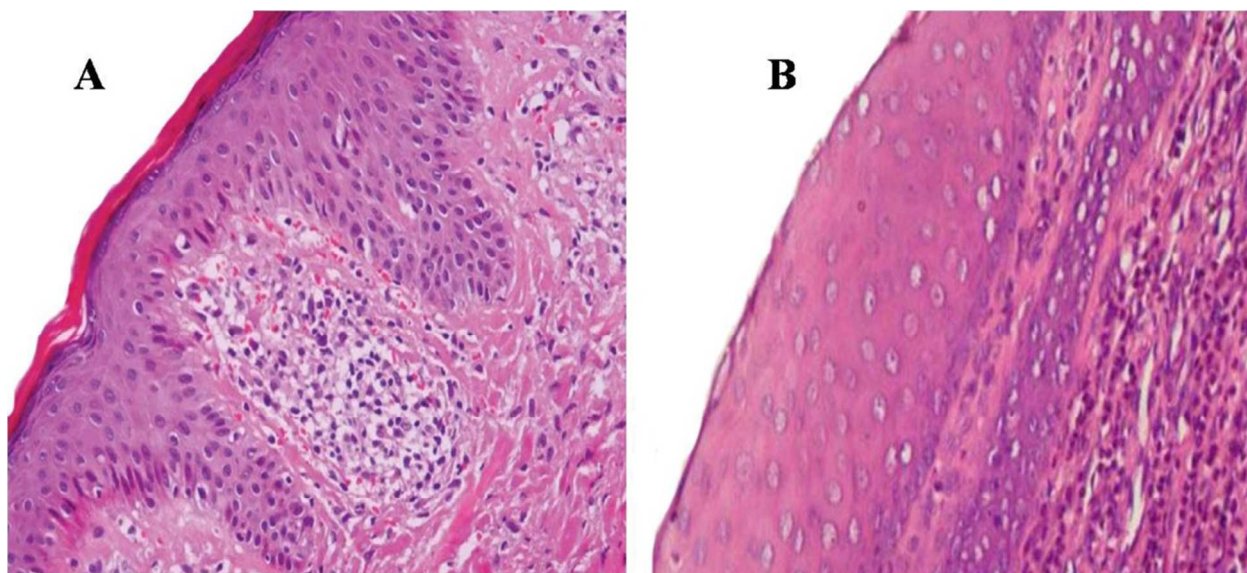
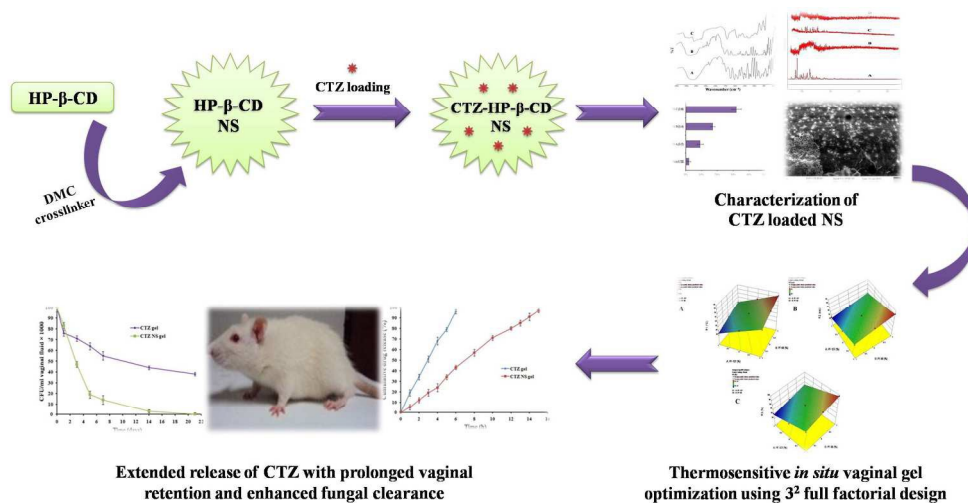


Fig. 10. Representative H and E (hematoxylin and eosin) stained histological slides of vaginal mucosa from female Wistar albino rats (A) Inflammatory condition with extensive neutrophil accumulation in lamina propria of the vaginal squamous epithelium and (B) Non-inflammatory vaginal mucosa in high view appearance (magnification: X200).



408x203mm (300 x 300 DPI)